Vietnam Journal of Earth Sciences, 42(1), 93–104, Doi: 10.15625/0866-7187/42/1/14761

(VAST)

Vietnam Academy of Science and Technology

Vietnam Journal of Earth Sciences

http://www.vjs.ac.vn/index.php/jse

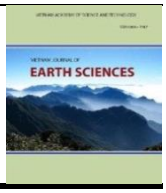

Pore water pressure accumulation and settlement of clays with a wide range of Atterberg's limits subjected to multi-directional cyclic shear

Tran Thanh Nhan[1,*] Hiroshi Matsuda[2]

[1]*University of Sciences, Hue University, 77 Nguyen Hue, Hue, Vietnam*
[2]*Yamaguchi University, 2-16-1 Tokiwadai, Ube, Yamaguchi, 755-8611, Japan*

Received 12 August 2019; Received in revised form 27 November 2019; Accepted 17 December 2019

ABSTRACT

In this study, normally consolidated specimens on four clays with a wide range of Atterberg's limits were tested by applying several series of undrained multi-directional cyclic shear followed by drainage. The cyclic shear tests were carried out under the shear strain amplitudes (γ = 0.05%-2.00%), number of cycles n = 200 and the phase difference θ = 90°. Then the accumulation of cyclic shear-induced pore water pressure and the post-cyclic settlement in strain (ε_v, %) were observed and discussed. In conclusion, it is clarified that the pore water pressure ratio (U_{dyn}/σ'_{vo}) increases with γ and the soils with higher Atterberg's limits show lower U_{dyn}/σ'_{vo}, and under the multi-directional cyclic shear strain at γ > 0.4%, Hue clay and Kaolinite clay with relatively low plasticity suffer from cyclic failure. In addition, the post-cyclic settlement has a tendency of decreasing with the Atterberg's limits in the range of plasticity index from I_p = 25.5 to 63.8, meanwhile when I_p < 25.5, different tendencies were observed e.g., Hue clay (with lower I_p) shows a smaller settlement compared with those on Kaolin (with higher I_p). Furthermore, the threshold number of cycles (n_{tp}) and cumulative shear strain (G^*_{tp}) for pore water pressure buildup were then clarified.

Keywords: Atterberg's limits, cyclic shear; pore water pressure; post-cyclic settlement.

1. Introduction

In the coastal area, soil deposits are subjected to horizontal cyclic shear deformation due to such as ocean waves, earthquakes, pile drivings, etc. In such soil deposits, although clayey soils show higher cyclic shear resistance compared with sand when subjected to undrained cyclic shear for short-term loading, for the case of long-term loading cyclic shear-induced failure would occur for normally consolidated and over-consolidated clays (Andersen et al., 1976; Yasuhara and Andersen, 1991). Such a failure of clayey soils has been confirmed through laboratory tests (Yasuhara and Andersen, 1991; Nhan et al., 2012; Nhan, 2013) as well as *in situ* records (Sasaki et al., 1980; Mendoza and Auvinet, 1988). Even in the case of no failure, the pore water pressure may accumulate to a relatively high level leading to considerable cyclic degradation of the soils (Yasuhara and Andersen, 1991; Ohara et al., 1984; Nhan et al., 2015).

*Corresponding author, Email: ttnhan@hueuni.edu.vn

Furthermore, the dissipation of cyclic shear-induced pore water pressure results in additional settlements which have been obviously recorded after the earthquakes (Zeevaert, 1983; Suzuki, 1984; Matsuda, 1997).

For cohesive soils, dynamic properties have been studied (Andersen et al., 1976; Yasuhara and Andersen, 1991; Suzuki, 1984; Fujiwara et al., 1985, 1987; Ohara and Matsuda, 1988; Yasuhara et al., 1992; Hyde et al., 1993), in which effects of cyclic loading conditions such as loading duration, frequency, and intensity have been observed (Fujiwara et al., 1985). Recently, the direction of cyclic loading and the Atterberg's limits have been confirmed to be important factors governing the cyclic shear-induced pore water pressure accumulation and settlement of soil deposits (Nhan et al., 2016, 2017; Nhan and Matsuda, 2017). Therefore, the effect of the multi-directional cyclic shear on such properties should be clarified furthermore.

In this study, several series of multi-directional cyclic simple shear tests were carried out on normally consolidated clay specimens under undrained condition and the pore water pressure accumulation during undrained cyclic shear and the settlement after cyclic shear were observed and based on which, effects of the multi-directional cyclic shears on such properties were then discussed in connection with those of the Atterberg's limits of clayey soils.

2. Experimental aspects

2.1. Test specimens

In this study, four kinds of clayey soils were used. The first soil is soft soil of the Phu Bai formation (amb$Q_2^{1\text{-}2}$ *pb*) which spreads widely along the coastal area in Thua Thien Hue and Quang Tri province. In Hue city and surrounding areas, such soils are stratified close to the ground surface and therefore the stability of structures and its economic efficiencies are considerably affected by the disadvantageous engineering properties. The soil sample (hereinafter called as Hue clay) was collected from boreholes in Hue city and used for the cyclic shear tests.

In addition, two natural clays named as Kitakyushu clay and Tokyo bay clay which were collected from seabed in Japan, and Kaolinite clay which is a standardized clay produced in Japan were also used. Index properties of samples are shown in Table 1, and the grain size distribution curves and *e*-log*P* curves are shown in Figs. 1 and 2, respectively.

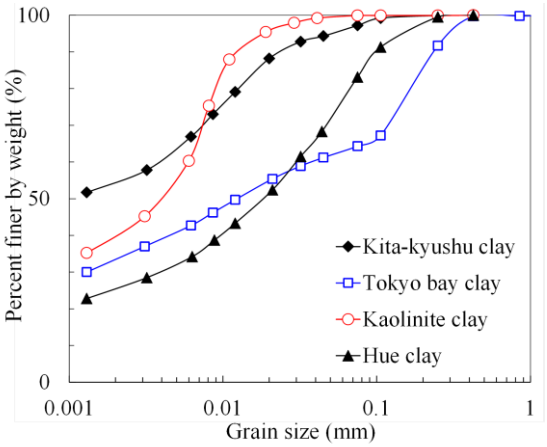

Figure 1. Grain size distribution curves of tested samples

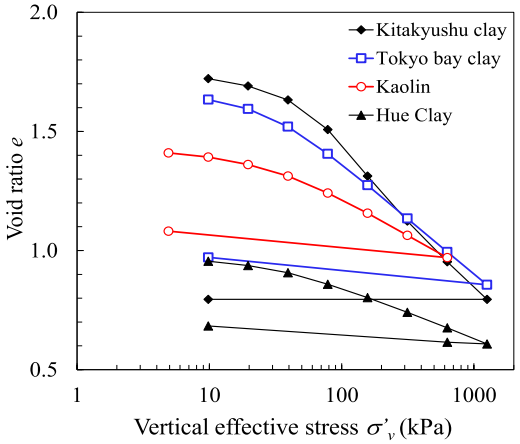

Figure 2. e-log*P* curves of tested samples

Table 1. Index properties of tested samples

Property	Kitakyushu clay	Tokyo bay clay	Kaolin	Hue clay
Specific gravity, G_s	2.63	2.77	2.71	2.68
Liquid limit, w_L (%)	98.0	66.6	47.8	29.4
Plastic limit, w_P (%)	34.2	25.0	22.3	18.7
Plasticity index, I_p	63.8	41.6	25.5	10.7
Compression index C_c	0.60	0.46	0.31	0.20
Swelling index C_s	0.00	0.05	0.05	0.04

2.2. Test procedures and conditions

In this study, the cyclic shear tests were carried out by the multi-directional cyclic simple shear test apparatus which was developed at Yamaguchi University (Japan) and used for researches related to the dynamic behaviours of clays and sands (Nhan et al., 2012, 2015, 2016, 2017; Nhan, 2013; Matsuda, 1997; Nhan and Matsuda, 2017). In order to prepare test specimens, the soils were firstly mixed with de-aired water to form slurry having water content of about $1.5 \times w_L$ where w_L is the liquid limit. Secondly, the slurry of each clay was kept for one day under the constant water content. The slurries were then de-aired in the vacuum cell before pouring into the Kjellman-type shear box. The membrane-enclosed specimen was prevented from lateral expansion by a stack of acrylic rings. The slurry was then pre-consolidated under the vertical stress of σ_{vo} = 49 kPa until the pore water pressure at bottom surface of the specimen was dissipated. Since the cyclic shear tests were required to be performed under the undrained condition, the saturation of specimen was confirmed as *B*-value > 0.95.

Following the pre-consolidation, soil specimens with the dimensions of 75 mm in diameter and 20 mm in height were subjected to undrained multi-directional cyclic shear for the number of cycles as n = 200, shear strain amplitudes in the range from γ = 0.05% to 3.0% and the phase difference of θ = 90° which is known as gyratory cyclic shearing. The cyclic shear was sinusoidal with the period of 2.0 s. Following the undrained cyclic shear, drainage was allowed from the top surface of the specimen. The pore water pressure at the bottom surface and the settlement were measured with time until the dissipation of the pore water pressure at the bottom surface of soil specimen was confirmed. The conditions of undrained cyclic shear tests are shown in Table 2.

Table 2. Conditions for undrained multi-directional cyclic shear test

Sample	Kitakyushu clay	Tokyo bay clay	Kaolin	Hue clay
Shear strain amplitude, γ (%)	0.05 - 2.15	0.05 - 1.97	0.10 - 2.03	0.05 - 1.94
Consolidation stress, σ'_{vo} (kPa)	49			
Number of cycles, n	200			
Phase difference, θ (°)	90			

3. Results and discussions

3.1. Pore water pressure accumulated in saturated clays

Typical changes of pore water pressure ratio (Nhan et al., 2016, 2017), defined by U_{dyn}/σ'_{vo} where U_{dyn} is the cyclic shear-induced pore water pressure and σ'_{vo} is initial effective stress, are shown in Figs. 3a, b, c, d for Kitakyushu clay, Tokyo bay clay, Kaolin and Hue clay, respectively. It is seen that U_{dyn}/σ'_{vo} increases with the number of cycles (n) and at the same n, cyclic shears with larger shear strain amplitude (γ) induce higher U_{dyn}/σ'_{vo}. For Kaolin and Hue clay which show relatively low Atterberg's limits, U_{dyn}/σ'_{vo} considerably increases regardless of

γ and when $\gamma \geq 0.4\%$, U_{dyn}/σ'_{vo} may approach $U_{dyn}/\sigma'_{vo} = 0.8$ which has been considered as a criterion for cyclic failure of cohesive soils (Andersen et al., 1976; Nhan et al., 2012; Nhan, 2013). Meanwhile for Kitakyushu clay and Tokyo bay clay, U_{dyn}/σ'_{vo} fluctuates around zero when $\gamma \approx 0.1\%$ even after long-term application of cyclic shear strain.

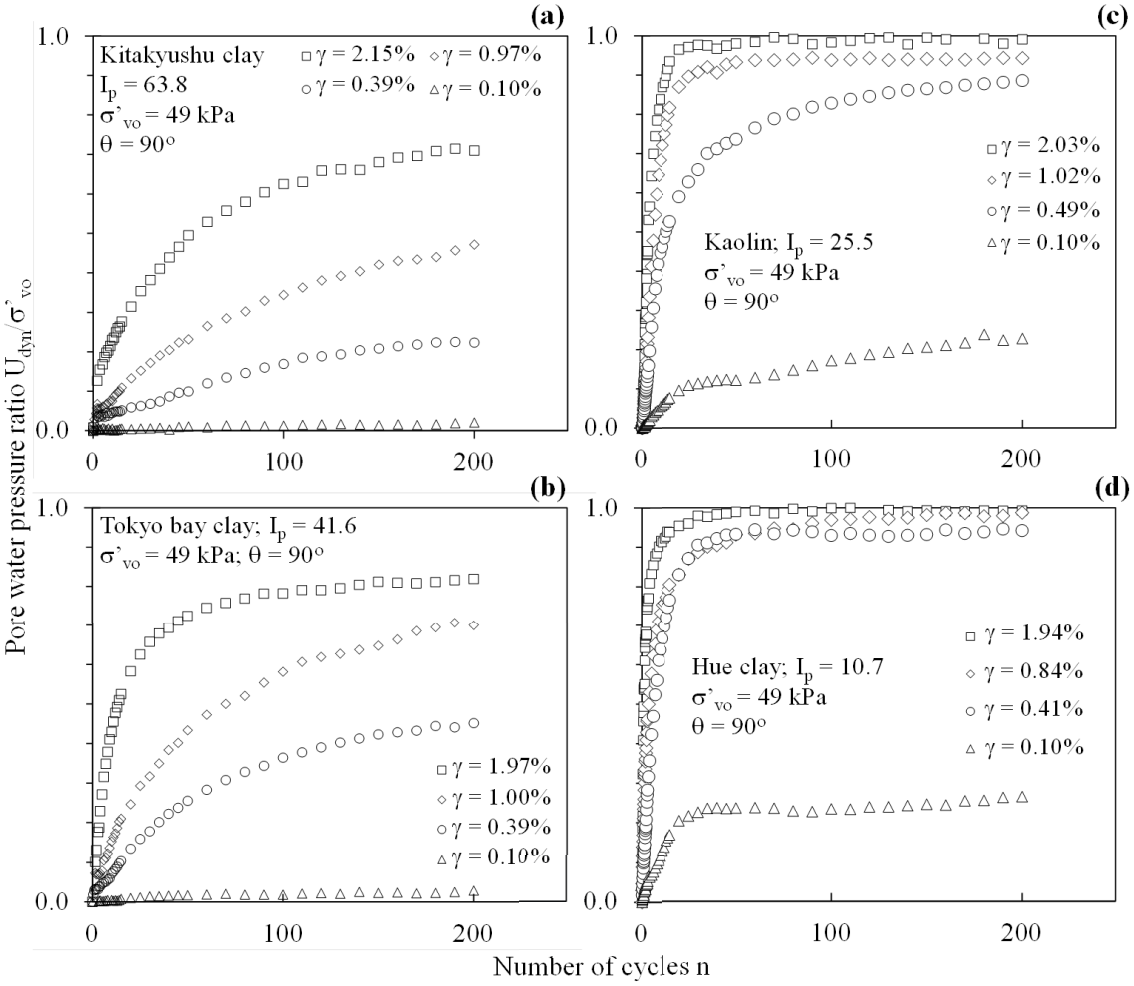

Figure 3. Pore water pressure accumulated in saturated clays subjected to undrained multi-directional cyclic shear at various shear strain amplitudes

Relationships between U_{dyn}/σ'_{vo} and γ are shown in Fig. 4 for each clay subjected to undrained multi-directional cyclic shear with $\theta = 90^o$ and $n = 200$. Increasing tendencies of U_{dyn}/σ'_{vo} with γ are seen for all clayey soils and at the same γ (and also at the same n, γ and θ), the soils with higher Atterberg's limits show lower U_{dyn}/σ'_{vo}. Then, the relation of $U_{dyn}/\sigma'_{vo} > 0.8$ can be confirmed for Kaolin and Hue clay when $\gamma > 0.4\%$. Therefore, the observations indicate that the Atterberg's limit significantly affects the cyclic shear-induced pore water pressure accumulation and that, for clays with relatively low plasticity such as Kaolin and Hue clay, cyclic failure potential should be considered under strong dynamic loading (*e.g.* $\gamma > 0.4\%$).

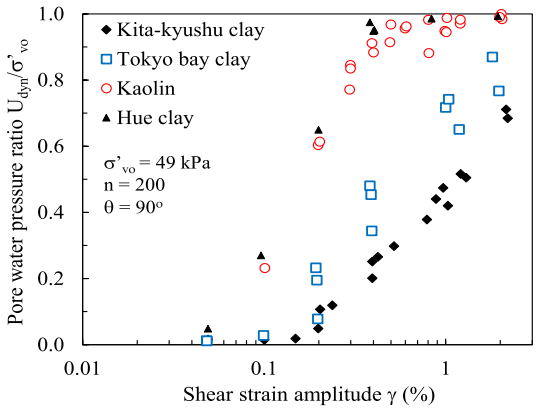

Figure 4. Relations between U_{dyn}/σ'_{vo} and γ for clays with a wide range of Atterberg's limits subjected to undrained multi-directional cyclic shear

3.2. Relations between the pore water pressure ratio and cumulative shear strain

In order to observe the accumulation of cyclic shear-induced pore water pressure in saturated clays, the cumulative shear strain (G^*) was incorporated (Fukutake and Matsuoka, 1989). This is a new strain path parameter denoting the length of shear strain path during cyclic shear. G^* is defined by Eq. (1) as follows:

$$G^* = \Sigma \Delta G^* = \Sigma (\Delta\gamma_x^2 + \Delta\gamma_y^2)^{0.5} \quad (1)$$

where $\Delta\gamma_x$ and $\Delta\gamma_y$ are the shear strain increment in two orthogonal directions, *i.e.* X and Y directions, respectively.

In this study, observed results of G^* are shown against γ by symbols in Fig. 5 for the multi-directional cyclic shear. A dashed line corresponds to calculated ones by using a relation of $G^* = 6.283 \times \gamma \times n$. Reasonable agreements are seen between the observed and calculated results and this suggests that in the case of $\theta = 90^o$, G^* can be obtained by the number of cycles n and the shear strain amplitude γ.

In order to show the applicability of G^* for describing the pore water pressure accumulation during multi-directional cyclic shear, observed results for U_{dyn}/σ'_{vo} in Figs. 3a, b, c and d are plotted against G^* in Figs. 6a, b, c and d, respectively. It is seen that, as a function of n and γ, G^* increases with γ when n is constant (n = 200) and that the larger the cumulative shear strain, the higher the ratio of pore water pressure. This observation suggests that the cyclic shear-induced pore water pressure accumulated in saturated clays with a wide range of Atterberg's limits can be expressed in terms of a function of G^*.

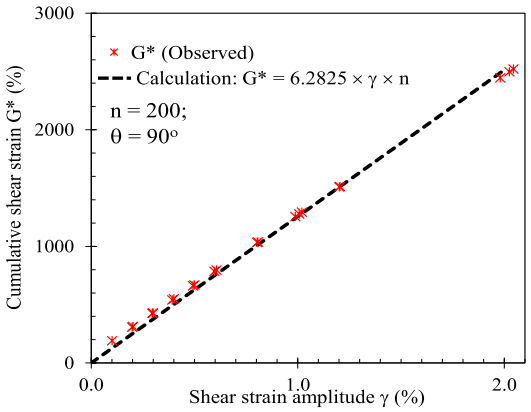

Figure 5. Relations between cumulative shear strain G* and shear strain amplitude γ for the multi-directional cyclic shear strain at $\theta = 90^o$ and $n = 200$

In Fig. 7, relationships between U_{dyn}/σ'_{vo} and G^* are shown for all clays under the cyclic shear conditions as mentioned before. It is seen that U_{dyn}/σ'_{vo} increases with G^* for each clay regardless of the conditions of cyclic shear. Similar advantage of G^* for eliminating the effect of cyclic shear direction on the pore water pressure accumulation has been confirmed for both clays and sands (Nhan, 2013; Nhan and Matsuda, 2017). Observed results in Fig. 7, however, indicate the discepancies of U_{dyn}/σ'_{vo} between clays and therefore, for the application of G^*, effects of the Atterberg's limit on the pore water pressure accumulation are still remained.

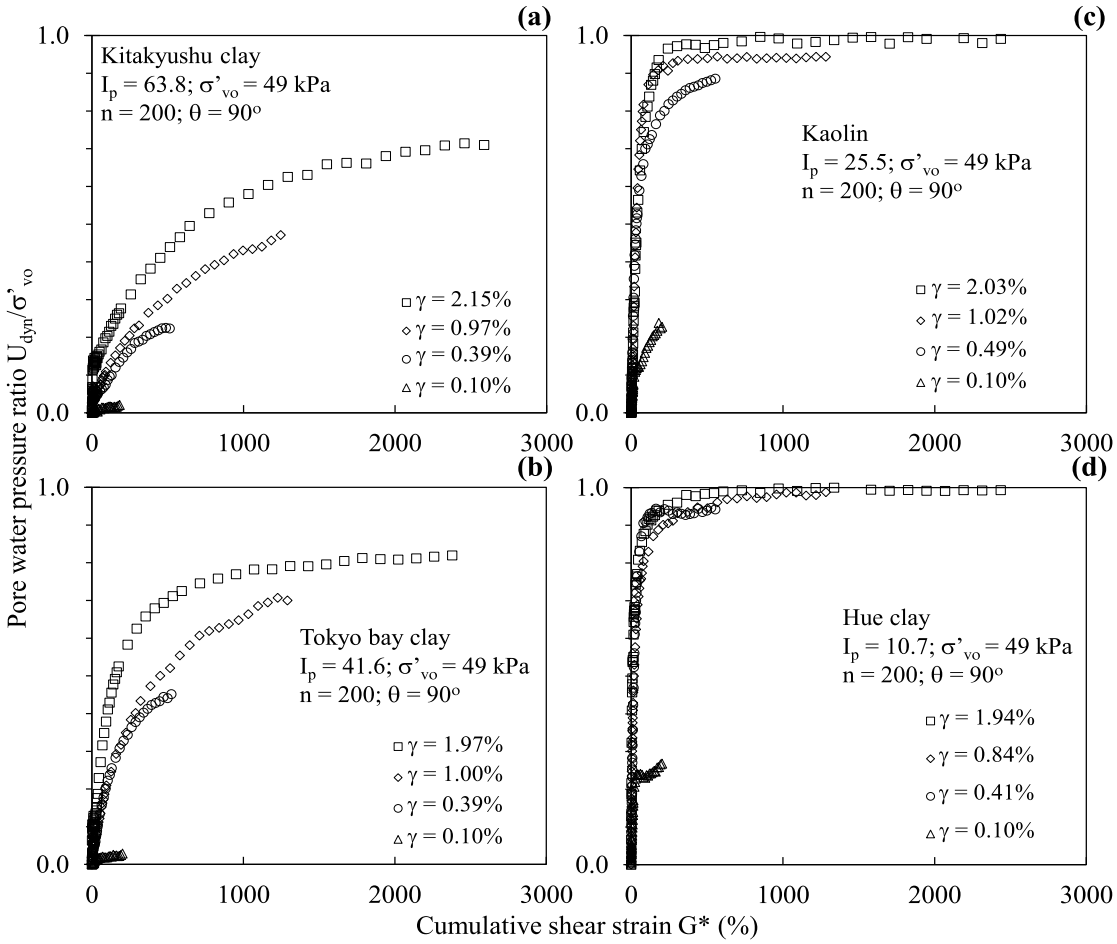

Figure 6. Relations between U_{dyn}/σ'_{vo} and G^* for clays with a wide range of Atterberg's limit subjected to undrained multi-directional cyclic shear at various shear strain amplitudes

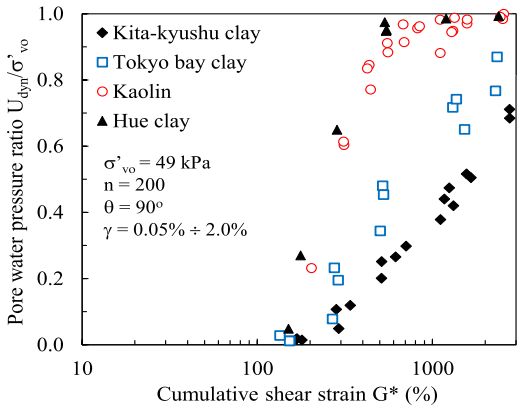

Figure 7. Relations between U_{dyn}/σ'_{vo} and G^* for clays with a wide range of Atterberg's limits subjected to undrained multi-directional cyclic shear

3.3. Threshold number of cycles and cumulative shear strain for pore water pressure buildup

When the amplitude of cyclic shear strain is smaller than a certain value, no pore water pressure buildup would be confirmed when cyclic loading stopped. The shear strain amplitude that divides the domains with no pore water pressure accumulation and significant accumulation is called the threshold shear strain amplitude (γ_{tp}). When the shear strain amplitude is larger than γ_{tp}, the cyclic shear-induced pore water pressure accumulates with the number of cycles (n). In contrast, when $\gamma < \gamma_{tp}$, such accumulation of

pore water pressure is negligible even after a large number of strain cycles (Hsu and Vucetic, 2006).

In order to show the generation of the pore water pressure during early stage of the cyclic shearing, experimental results in Figs. 3 and 6 were replotted against the logarithm of n and G^* as shown in Figs. 8, 9, respectively. It is seen that the number of cycles and cumulative shear strain at the time when the pore water pressure starts to increase can be obtained for the applied shear strain amplitude on each clay. These values are considered as threshold number of cycles and cumulative shear strain, and in this study, symbolized as n_{tp} and G^*_{tp} respectively.

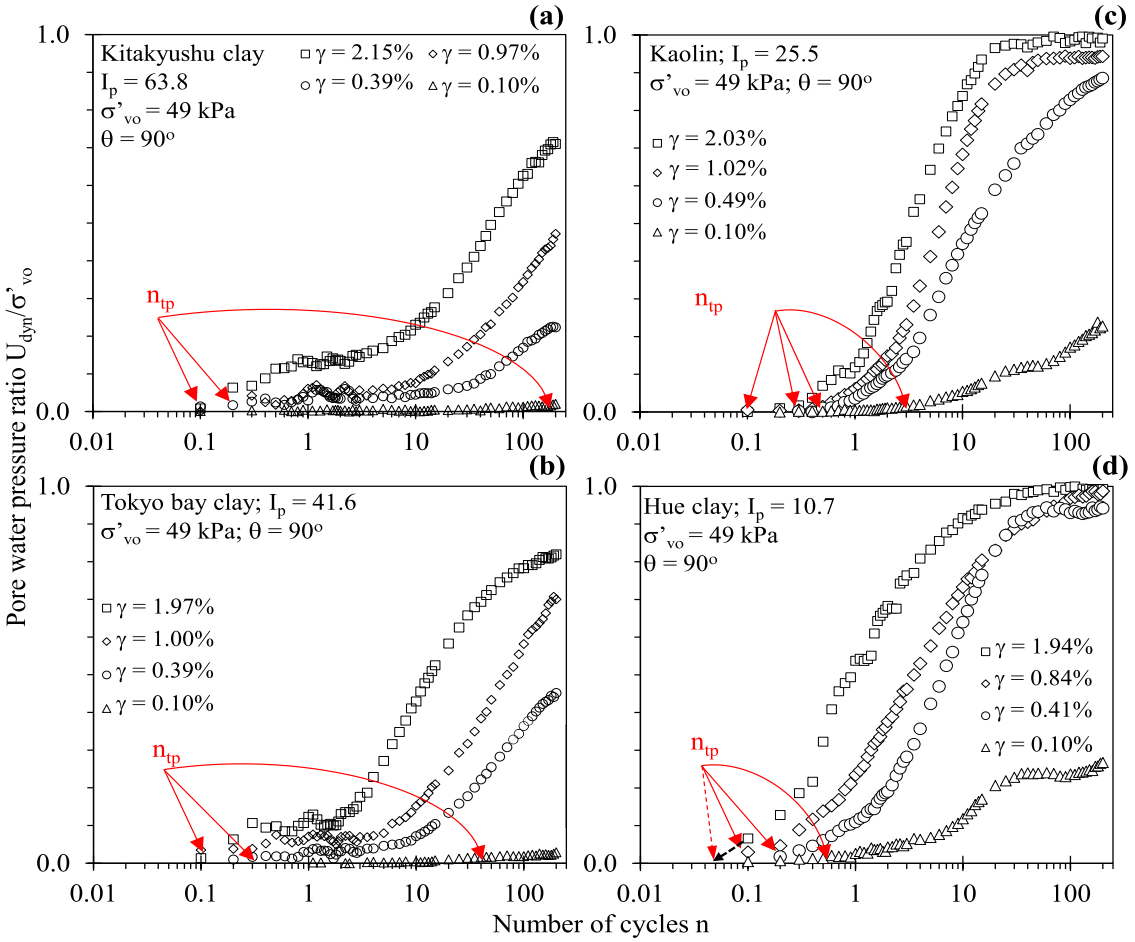

Figure 8. Changes in U_{dyn}/σ'_{vo} versus the logarithm of n for clays with a wide range of Atterberg's limits subjected to multi-directional cyclic shear at different shear strain amplitudes

The values of n_{tp} and G^*_{tp} are summarized in Table 3 and Fig. 10. It is seen that n_{tp} and G^*_{tp} generally increase with the increase in the Atterberg's limit but with the decrease in shear strain amplitude and that, such tendencies are seen only when $\gamma < 0.4\%$ and $I_p > 25.5$. For the case of $I_p < 25.5$ and $\gamma \geq 0.4\%$, *i.e.* when clays with relatively low plasticity such as Hue clay and Kaolin are subjected to relatively strong cyclic loading, the pore water pressure generates and accumulates quickly, then very small values for n_{tp} and G^*_{tp} are obtained.

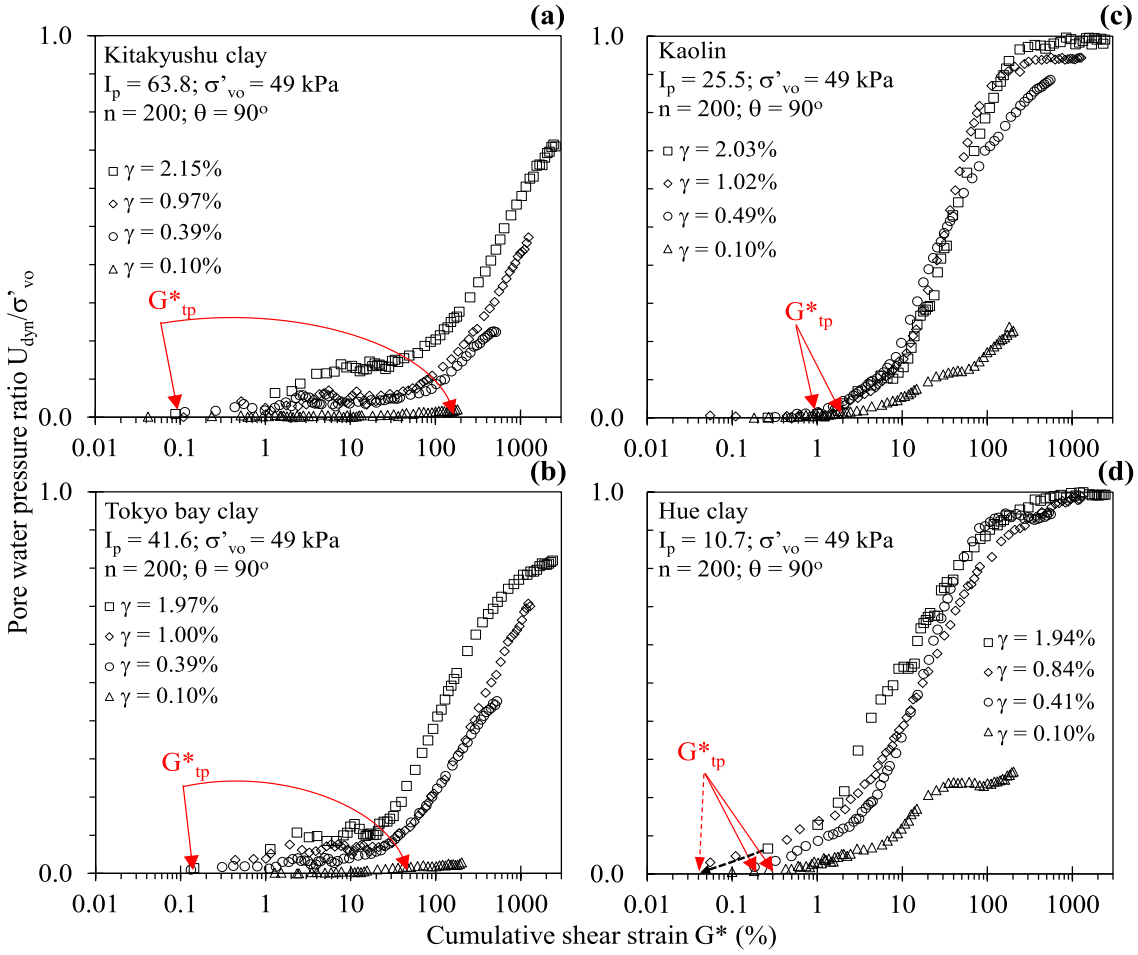

Figure 9. Changes in U_{dyn}/σ'_{vo} versus the logarithm of G^* for clays with a wide range of Atterberg's limits subjected to multi-directional cyclic shear at different shear strain amplitudes

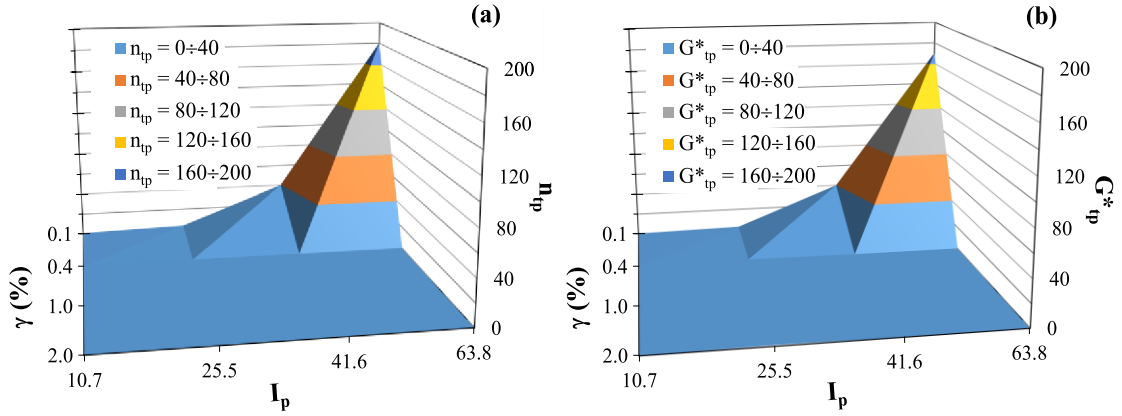

Figure 10. Changes in threshold number of cycles (n_{tp}) and cumulative shear strain (G^*_{tp}) for pore water pressure buildup with shear strain amplitude (γ) and plasticity index (I_p)

Table 3. Obtained values of n_{tp} and G^*_{tp} for different clays and shear strain amplitudes

Soil	Threshold number of cycles (n_{tp})				Threshold cumulative shear strain (G^*_{tp},%)			
	γ ≈ 0.1 %	γ ≈ 0.4 %	γ ≈ 1.0 %	γ ≈ 2.0 %	γ ≈ 0.1 %	γ ≈ 0.4 %	γ ≈ 1.0 %	γ ≈ 2.0 %
Kitakyushu clay	180	0.2	0.1	0.1	170	0.1	0.1	0.1
Tokyo bay clay	40	0.3	0.1	0.1	40	0.13	0.13	0.13
Kaolinite clay	3	0.5	0.3	0.1	2	1.0	1.0	1.0
Hue clay	0.5	0.2	0.1	≈ 0.05	0.3	0.2	≈ 0.04	≈ 0.04

3.4. Post-cyclic settlement of clayey soils

Following the undrained cyclic shear, drainage was allowed from the top surface of specimen and the settlement was measured with time. The vertical settlements in strain (ε_v, %) are typically plotted against elapsed time in Figs. 11a, b, c, d for Kitakyushu clay, Tokyo bay clay, Kaolin and Hue clay, respectively.

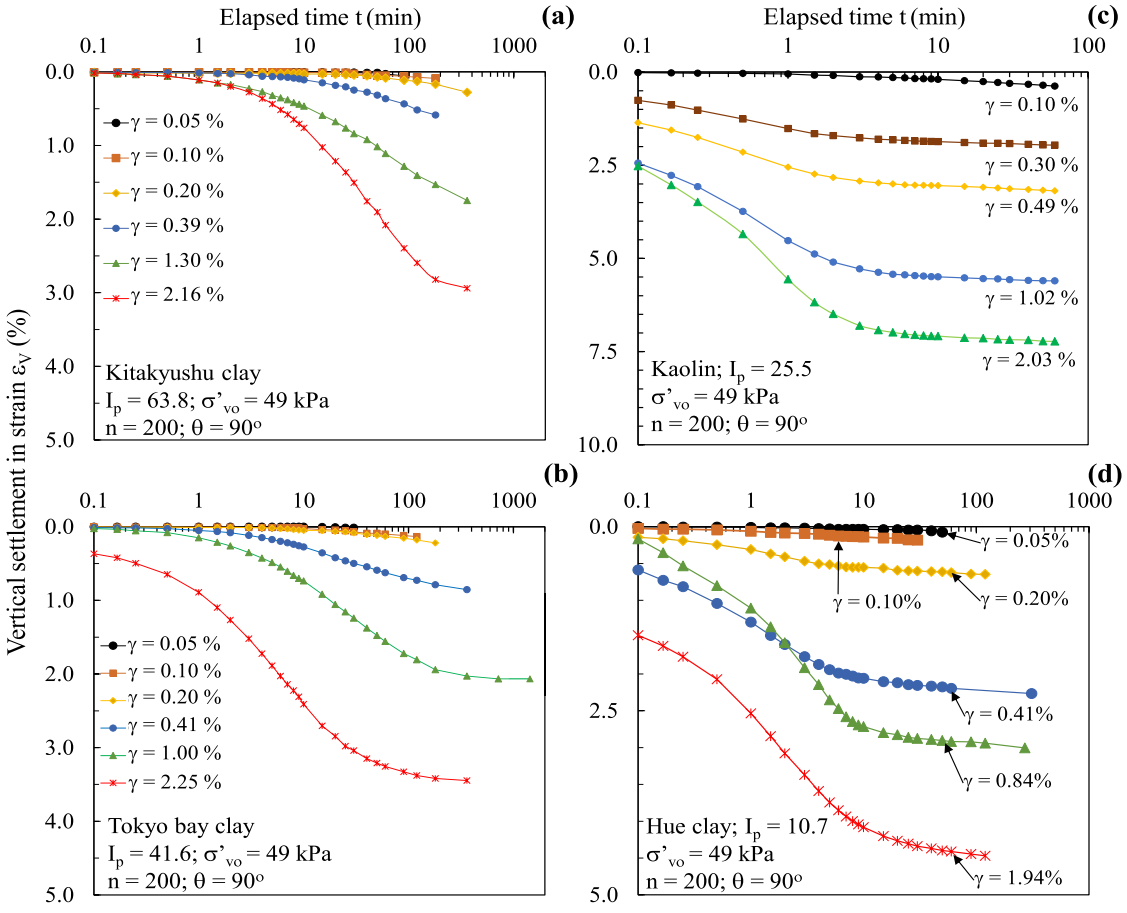

Figure 11. Settlement-time relations of clays with a wide range of Atterberg's limits under multi-directional cyclic shear with different shear strain amplitudes

It is seen that the larger the shear strain amplitude the higher the settlement of clayey layer. The observed results of ε_v were also plotted against γ in Fig. 12(a) and G^* in Fig. 12(b). It is seen that ε_v increases with γ and G^* for clays with the plasticity index in the range from I_p = 25.5 to 63.8, and that the soils with higher plasticity show smaller post-

cyclic settlement. In Figs. 4 and 7, although the pore water pressures accumulated in Hue clay are slightly higher than those in Kaolin under the same cyclic shear condition, the settlement of Hue clay seems to be equal to those of Kaolin when $\gamma < 0.4\%$ and $G^* < 500\%$, as shown in Figs. 12a, b. For larger γ and G^*, different tendencies are seen showing smaller settlement on Hue clay compared with those on Kaolin. These observations suggest that the post-cyclic settlement on clay is affected not only by the level of the cyclic shear-induced pore water pressure but also by the compressibility of the soil which is affected by factors such as the content of fine-grains and the soil plasticity, etc.

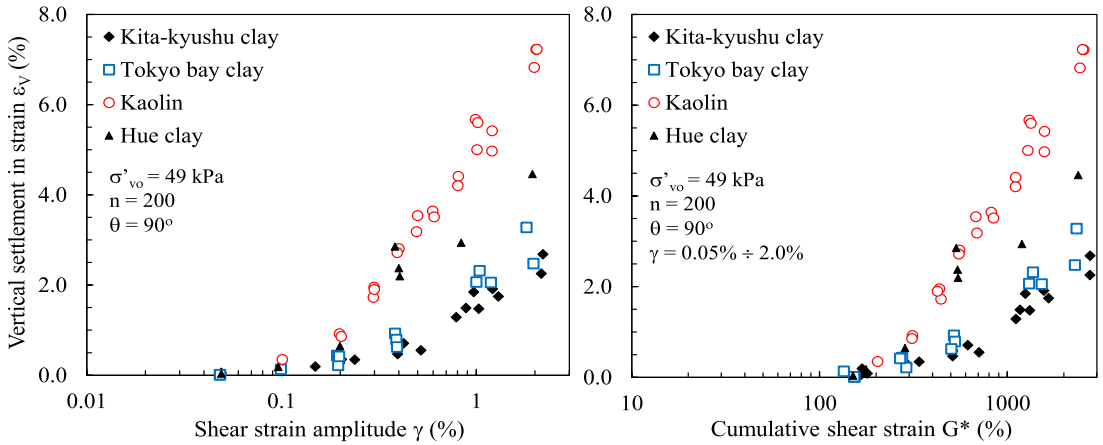

Figure 12. Relationships of the post-cyclic settlement versus shear strain amplitude and cumulative shear strain for clays with a wide range of Atterberg's limits

4. Conclusions

In this study, several series of multi-directional cyclic shear tests were performed on normally consolidated clays with a wide range of Atterberg's limits. The accumulation of pore water pressure during undrained cyclic shear and the settlement in the recompression stage after the cyclic shear were observed and discussed. The main conclusions are as follows:

Under the same cyclic shear conditions, clayey soils with higher Atterberg's limit show lower cyclic shear-induced pore water pressure. For the multi-directional cyclic shear at $\gamma > 0.4\%$, the pore water pressure ratio of Kaolin and Hue clay may reach $U_{dyn}/\sigma'_{vo} = 0.8$ and therefore, cyclic failure should be considered when the soils subjected to strong cyclic loading.

Relation of $G^* = 6.283 \times \gamma \times n$ was obtained for the multi-directional cyclic shear at the phase difference of $\theta = 90^o$.

Threshold values for the number of cycles (n_{tp}) and cumulative shear strain (G^*_{tp}) on the cyclic shear-induced pore water pressure buildup generally increase with the increase in the Atterberg's limit but decrease in the shear strain amplitude and such a tendency is evident when $\gamma < 0.4\%$ and $I_p \geq 25.5$. When $\gamma \geq 0.4\%$ and $I_p < 25.5$, the excess pore water pressure quickly increases and therefore very small values of n_{tp} and G^*_{tp} are obtained.

The cyclic shear-induced settlement increases with γ and G^* regardless of the Atterbeg's limit. For the range of I_p = 25.5 - 63.8, the soil with higher Atterberg's limit show smaller post-cyclic settlement. Meanwhile for smaller I_p, the settlement of Hue clay becomes equal to and smaller than those of Kaolinite clay.

Acknowledgements

This research is funded by Vietnam National Foundation for Science and Technology Development (NAFOSTED) under Grant Number 105.08-2018.01 and also by JSPS KAKENHI Grant Number 16H02362. The experimental works were also supported by the students who graduated Yamaguchi University. The authors would like to express their gratitude to them.

References

Andersen K.H., Brown S.F., Foss I., Pool J.H., Rosenbrand F.W., 1976. Effect of cyclic loading on clay behaviour. Proc. of Conf. Design and Construction of Offshore Structures. Institution of Civil Engineers, London, 75–79.

Fujiwara H., Yamanouchi T., Yasuhara K., Ue S., 1985. Consolidation of alluvial clay under repeated loading. Soils and Foundations, 25(3), 19–30.

Fujiwara H., Ue S., Yasuhara K., 1987. Secondary compression of clay under repeated loading. Soils and Foundations, 27(2), 21–30.

Fukutake K., Matsuoka H.A., 1989. Unified law for dilatancy under multi-directional simple shearing. J JSCE Div., C 412(III-1), 143–151 (in Japanese).

Hsu C.C., Vucetic M., 2006. Threshold shear strain for cyclic pore-water pressure in cohesive soils. Journal of Geotechnical and Geoenvironmental Engineering, 132(10), 1325–1335.

Hyde A.F.L., Yasuhara K., Hirao K., 1993. Stability criteria for marine clay under one-way cyclic loading. J. Geotechnical Eng., ASCE, 119(11), 1771–1788.

Matsuda H., 1997. Estimation of post-earthquake settlement-time relations of clay layers. Journal of JSCE Division C, JSCE, 568(III-39), 41–48 (in Japanese).

Mendoza M.J., Auvinet G., 1988. The Mexico Earthquake of September 19, 1985-Behaviour of building foundations in Mexico City. Earthquake Spectra, 4(4), 835–852.

Nhan T.T., Matsuda H., Thien D.Q., Tuyen T.H., An T.T.P., 2012. New criteria for cyclic failure of normally consolidated clays and sands subjected to uniform and irregular cyclic shear. Proc. of the International workshop Hue Geo-Engineering 2012, Vietnam, 127–138.

Nhan T.T., 2013. Study on excess pore water pressure and post-cyclic settlement of normally consolidated clay subjected to uniform and irregular cyclic shears. Doctoral dissertation, Yamaguchi University, Japan, 131pp.

Nhan T.T., Matsuda H., Hara H., Sato H., 2015. Normalized pore water pressure ratio and post-cyclic settlement of saturated clay subjected to undrained uni-directional and multi-directional cyclic shears. 10th Asian Regional Conference of IAEG, Kyoto, Japan, Tp3-16-1081481, 1–6.

Nhan T.T., Matsuda H., Sato H., 2016. A pore water pressure model for cyclic shear strain on clays, concerning the effects of cyclic shear duration and Atterberg's limits. The International Conference on Geotechnics for Sustainable Infrastructure Development - GEOTEC HANOI 2016, Hanoi, Vietnam, 1045–1054.

Nhan T.T., Matsuda H., 2017. Post-cyclic recompression of clays subjected to undrained cyclic shear. Geotechnical Frontiers 2017, Florida, USA, Geotechnical Special Publication (GSP281)-ASCE, 109–120.

Nhan T.T., Matsuda H., Sato H., 2017. A model for multi-directional cyclic shear-induced pore water pressure and settlement on clays. Bulletin of Earthquake Engineering, 15(7), 2761–2784.

Ohara S., Matsuda H., Kondo Y., 1984. Cyclic simple shear tests on saturated clay with drainage. Journal of JSCE Division C, JSCE, 352/III-2, 149–158 (in Japanese).

Ohara S., Matsuda H., 1988. Study on the settlement of saturated clay layer induced by cyclic shear. Soils and Foundations, 28(3), 103–113.

Sasaki Y., Taniguchi E., Matsuo O., Tateyama S., 1980. Damage of soil structures by earthquakes. Technical Note of PWRI, 1576, Public Works Research Institute (in Japanese).

Suzuki T., 1984. Settlement of saturated clays under dynamic stress history. Journal of the Japan Society of Engineering Geology, 25(3), 21–31 (in Japanese).

Yasuhara K., Andersen K.H., 1991. Recompression of normally consolidated clay after cyclic loading. Soils and Foundations, 31(1), 83–94.

Yasuhara K., Hirao K., Hyde A.F.L., 1992. Effects of cyclic loading on undrained strength and compressibility of clay. Soils and Foundations, 32(1), 100–116.

Zeevaert L., 1983. Foundation engineering for difficult subsoil conditions. Van Nostrand Co. Ltd (2nd Edition), New York, USA.